Journal of Applied Polymer Science

Crystallization and melting behavior of partially miscible six-armed poly(L-lactic acid)/poly(3-hydroxybutyrate-co-3-hydroxyvalerate) blends

Ni Jiang, Hideki Abe
Bioplastic Research Team, Biomass Engineering Program Cooperation Division, RIKEN Center for Sustainable Resource Science, 2-1, Hirosawa, Wako-Shi, Saitama 351-0198, Japan
Correspondence to: H. Abe (E-mail: habe@riken.jp)

ABSTRACT: The crystallization kinetics and spherulitic morphology of six-armed poly(L-lactic acid) (6a-PLLA)/poly(3-hydroxybutyrate-*co*−3-hydroxyvalerate) (PHBV) crystalline/crystalline partially miscible blends were investigated with differential scanning calorimetry and polarized optical microscopy in this study. Avrami analysis was used to describe the isothermal crystallization process of the neat polymers and their blends. The results suggest that blending had a complex influence on the crystallization rate of the two components during the isothermal crystallization process. Also, the crystallization mechanism of these blends was different from that of the neat polymers. The melting behavior of these blends was also studied after crystallization at various crystallization temperatures. The crystallization of PHBV at 125°C was difficult, so no melting peaks were found. However, it was interesting to find a weak melting peak, which arose from the PHBV component for the 20/80 6a-PLLA/PHBV blend after crystallization at 125°C, and it is discussed in detail. © 2015 Wiley Periodicals, Inc. J. Appl. Polym. Sci. **2015**, *132*, 42548.

KEYWORDS: biopolymers and renewable polymers; blends; differential scanning calorimetry (DSC); morphology

Received 25 March 2015; accepted 26 May 2015
DOI: 10.1002/app.42548

INTRODUCTION

The focus on environmental issues and depleting fossil resources has led to increased studies of renewable-resource-based products for industrial applications.[1,2] The polyesters poly(L-lactic acid) (PLLA) and poly(3-hydroxybutyrate-*co*−3-hydroxyvalerate) (PHBV) can be produced from renewable resources, and they are biodegradable and biocompatible crystalline polymers. Both of them have comparable thermal and mechanical properties to those of commercial polymers. However, the application of these materials is hindered by their narrow processing windows, poor thermal stabilities, high brittleness, and so on. Thus, both chemical and physical methods have been proposed to improve their properties.[3–7]

Polymer blending is a useful and convenient physical methods for enhancing the properties of polymers. Therefore, it is significant to study the physical properties of the biodegradable crystalline/crystalline PLLA/PHBV blends. It is known that the processing and final properties of crystalline polymer blends is determined in part by their melting and crystallization behaviors. So, the investigation of the kinetics of crystallization and the melting behavior of polymer blends is necessary from both theoretical and practical perspectives. The crystallization behavior of two crystalline components in these blends is particularly interesting because it involves the crystallization of two different polymers, each within its specific temperature regime.[8] It depends on both the miscibility and thermal properties [glass-transition temperature (T_g), melting temperature (T_m), etc.] of the two components and the crystallization conditions.[9]

The miscibility of poly(3-hydroxybutyrate) (PHB)/PLLA blends has been extensively studied.[10,11] It was found that the miscibility is strongly dependent on the molecular weight of the PLLA component. Blümm and Owen[12] reported that low-molecular-weight PLLA [number-average molecular weight (M_n) = 1759] was miscible with PHB in the melt over the whole composition range, whereas a blend of high-molecular-weight PLLA (M_n = 159400) with PHB showed biphasic separation. It could be deduced from this fact that the miscibility of PLLA with PHBV, the copolymer of PHB, may have also depended on the molecular weight of the PLLA component. In addition, the crystallization behavior of the crystalline/crystalline blends largely depended on the difference between the T_m's of the two components. When the T_m difference was large, the component with a higher T_m crystallized first, and the lower T_m component crystallized at a lower temperature in limited regions. When the difference in T_m was small enough, the two components had a high possibility of crystallizing simultaneously.[13] For the PLLA/PHBV blends, the difference in T_m was small, so simultaneous crystallization was possible for these blends.

The dominant processes for crystallization from the molten state are nucleation and subsequent crystal growth; this is mainly influenced by the temperature, pressure, and time. The crystallization kinetics can be analyzed by means of isothermal techniques, in which the crystallization process is specifically investigated at defined temperatures. A well-known description of the crystallization process is the Avrami phase-transition theory.[14,15] According to previous studies,[16,17] partially miscible six-armed PLLA (6a-PLLA)/PHBV blends showed different spherulitic morphologies after crystallization at different temperatures. At lower temperatures, only the PHBV component could crystallize, and banded spherulites with positive birefringence were found. At intermediate temperatures, both components crystallized simultaneously, and interpenetrating spherulites were found. However, at higher temperatures, it was difficult for the PHBV component to crystallize, and only negative PLLA spherulites were found. In addition, the miscibility of the blends played an important role in determining the spherulitic morphologies because of the different phase structure.

In this study, to elucidate the effect of one component on the crystallization kinetics, morphology, and melting behavior of the other component in partially miscible 6a-PLLA/PHBV blends, the isothermal crystallization and subsequent melting of these blends were investigated with differential scanning calorimetry (DSC) and polarized optical microscopy (POM). The crystallization mechanism of these blends at different temperatures was examined in detail, and the melting peaks were well identified.

EXPERIMENTAL

6a-PLLA ($M_n = 33{,}100$, polydispersity index = 1.5, $T_g = 57.3$°C, $T_m = 175$°C) was synthesized by ring-opening polymerization according to a reported method.[16] The L-lactide monomer (Purac Co., recrystallized from toluene solution under isothermal condition at 65°C), diethyl zinc catalyst, dichloromethane solvent, and D-mannitol initiator, which had six hydroxyl groups, were placed into a reactor inside the glovebox. Polymerization was carried out at 40°C under sealed conditions for 3 days. The produced polymer was dissolved in chloroform and precipitated in methanol. The precipitate was dried *in vacuo* at 50°C. To remove the residual Zn compounds in the product, chloroform solutions of polymers (0.5% w/v) were washed with acetic acid three times and then precipitated in methanol. PHBV ($M_n = 149{,}300$, polydispersity index = 2.3, $T_g = -2.8$°C, $T_m = 151$°C, hydroxyvalerate (HV) content = 12 mol %, ICI, Agricultural Division, Billingham, United Kingdom, trade name Biopol) was purified by dissolution in chloroform at 80°C and then precipitation from methanol at ambient temperature.

The 6a-PLLA/PHBV blends were prepared by solution casting with chloroform as a mutual solvent. The films for POM measurement were prepared by solution casting (25 mg/mL) on a glass slide. The solvent was allowed to evaporate in a fuming hood first and then *in vacuo*. Compositions of 20/80, 40/60, 60/40, and 80/20 w/w (where the first number is the amount of 6a-PLLA component) were prepared.

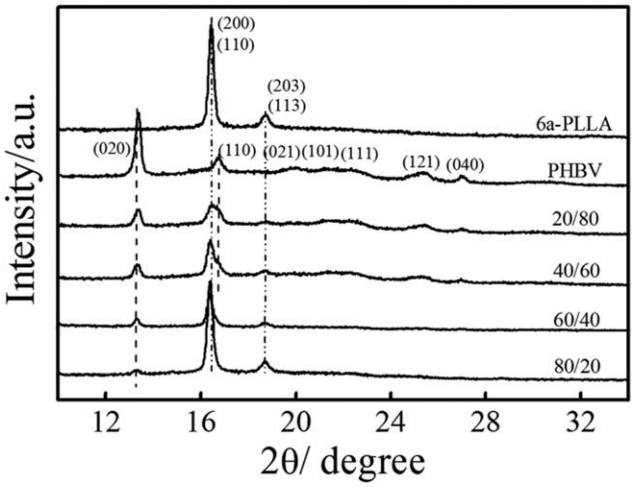

Figure 1. WAXD patterns of the 6a-PLLA/PHBV blends crystallized at 79°C.

The wide-angle X-ray diffraction (WAXD) patterns of these films were recorded at room temperature on a Rigaku RINT2500 diffractometer with nickel-filtered Cu Kα radiation ($\lambda = 0.154$ nm, 40 kV, and 100 mA) in the 2θ range of 5–35° with a scanning step of 0.02° and a scanning rate of 1°/min. The isothermal crystallization and melting process of samples were measured by DSC. Samples were analyzed with a PerkinElmer Pyris 1 equipped with a cooling accessory under a nitrogen flow of 20 mL/min. The samples maintained at 200°C were rapidly quenched to the crystallization temperature (T_c) and kept there for different times; then, they were heated to 200°C at different heating rates (5, 20, and 60°C/min). The crystalline morphologies of the 6a-PLLA/PHBV blends were observed under crossed polarizers with an optical microscope (Olympus BX53) equipped with a Linkam hot stage. The samples were first melted at 200°C for 2 min to erase any thermal history and then quickly moved to the hot-stage setting at T_c.

RESULTS AND DISCUSSION

Crystal Structure

6a-PLLA and PHBV were already proven to be partially miscible blends in our previous study. Also, interpenetrating spherulites were formed in these blends in a certain temperature range; that is, the lamellae of both components were interlocked by each other.[16] It was necessary to investigate the effect of blending on the crystal structure of the two components before the crystallization kinetic study. Figure 1 shows the WAXD patterns of the neat 6a-PLLA, neat PHBV, and various 6a-PLLA/PHBV blends after crystallization at 79°C, the temperature at which both components could crystallize. PHBV showed diffraction peaks at 13.5 and 16.8°, which corresponded to the (020) and (110) planes, and three weak peaks at 19.1, 22.2, and 25.5°. This indicated that there was only a PHB-type lattice existing in PHBV because of the lower content of HV units. Similar results were reported in the literature for PHBV copolymers.[18] For the 6a-PLLA sample, two strong reflections located at 16.4 and 18.7° were found; this indicated the formation of α′ form crystals.[19] The characteristic peaks of the series of 6a-PLLA/PHBV

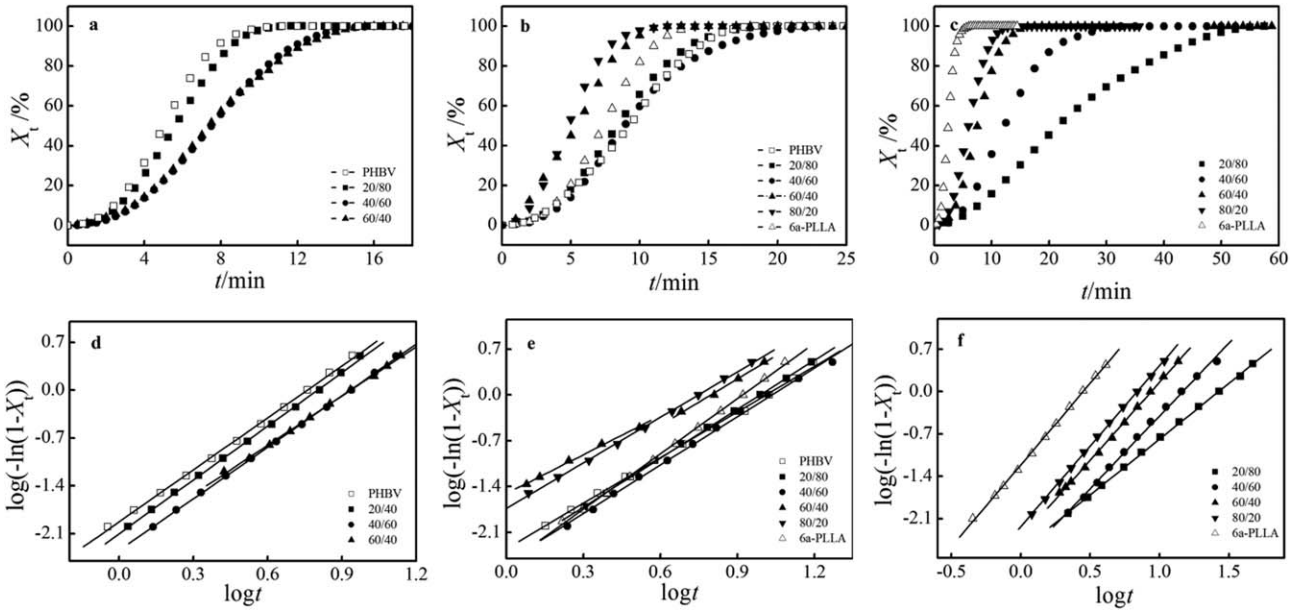

Figure 2. Plots of X_t versus time and the Avrami plots of the 6a-PLLA/PHBV blends at different crystallization temperatures: (a,d) 50, (b,e) 79, and (c,f) 125°C.

blends were similar to those of neat 6a-PLLA and PHBV, and the intensity of the diffraction peaks of one component decreased with increasing content of the other one. No new characteristic peaks appeared in the WAXD patterns; this suggested that blending had no obvious effect upon the crystal structure of each component.

Isothermal Crystallization Kinetics and Morphology

The crystallization conditions played dominate roles in determining the final microstructure of the crystalline polymers and their blends. For the 6a-PLLA/PHBV blends, three different T_cs were chosen for the crystallization kinetics and morphological study, that is, a lower T_c of 50°C at which 6a-PLLA could not crystallize, an intermediate T_c of 79°C at which both components could crystallize, and a higher T_c of 125°C at which the crystallization of the PHBV component was difficult.

The isothermal crystallization of the neat 6a-PLLA, neat PHBV, and 6a-PLLA/PHBV blends was studied in detail by DSC analysis. Typical crystallization isotherms, which were obtained by the plotting of the relative crystallinity (X_t) versus crystallization time (t), are shown in Figure 2(a–c). The characteristic sigmoidal isotherms shifted right along the time axis with increasing content of the other component at 50 and 125°C, and the whole t also increased with the content of the other component. At 79°C, the crystallization was a little complicated because both components could crystallize at this temperature. An important parameter describing the crystallization rate is the crystallization half-time ($t_{1/2}$); this is the time at which the extent of crystallization was 50%. It could be extracted directly from the plot of X_t versus time, as shown in Table I. It was obvious that the $t_{1/2}$ value of one component increased gradually with an increase in the content of the other component at lower and higher temperatures; this indicated that the overall crystallization rate decreased with an increasing in the content of the other component. It should be noted that the overall crystallization rate of the 60/40 blend was a little higher than that of 40/60 blend; this is discussed later. At 79°C, it was found that the overall crystallization rate of the 20/80 blend was higher than that of neat PHBV. When the content of 6a-PLLA was further increased to 40%, the overall crystallization rate decreased but was still higher than that of neat PHBV. The same tendency was found for the blend with a higher content of 6a-PLLA compared to neat 6a-PLLA. This was ascribed to the fact that the crystallization of the PHBV component was predominant in the blend with a lower 6a-PLLA content and vice versa. That is, the

Table I. Values of K, n, $t_{1/2}$, and G as a Function of T_c of the Neat 6a-PLLA, Neat PHBV, and Their Blends

T_c (°C)	Sample	$t_{1/2}$ (min)	n	$K \times 10^{-3}$ (min^{-1})	G (μm/min)
50	PHBV	5.03	2.5	11.85	8.1
	20/80	5.62	2.6	7.96	6.2
	40/60	7.51	2.5	4.55	5.1
	60/40	7.37	2.4	5.18	5.1
79	PHBV	9.28	2.3	4.48	23.6
	20/80	8.42	2.5	3.46	22.0
	40/60	8.91	2.5	2.81	20.2
	60/40	5.45	2.2, 2.4	—	20.1
	80/20	4.82	2.3	18.53	—
	6a-PLLA	7.37	2.8	2.57	—
125	20/80	21.65	1.8	2.35	3.5
	40/60	12.26	2.4	1.59	5.0
	60/40	7.52	2.6	3.76	9.1
	80/20	5.97	2.7	5.92	12.8
	6a-PLLA	2.4	2.7	61.48	8.6

introduction of one component facilitated the crystallization of the other one at the intermediate T_c.

The detailed isothermal crystallization processes of the polymers were analyzed on the basis of the Avrami equation as follows:

$$1-X_t=\exp(-Kt^n) \quad (1)$$

where K is the crystallization rate constant containing the nucleation and growth rates and n is the Avrami exponent. Equation (1) can be transformed into the usual double-logarithmic form:

$$\lg[-\ln\ (1-X_t)]=\ \lg K+n\lg t \quad (2)$$

According to eq. (2), the plot of $\lg[-\ln(1-X_t)]$ against $\lg t$ should yield a straight line, and n and K can be obtained from the slope and intercept, respectively. The double-logarithmic plots of the neat 6a-PLLA, neat PHBV, and 6a-PLLA/PHBV blends are represented in Figure 2(d–f). The results for the n and K values are also listed in Table I. All of the curves, except for those of 60/40 blend at 79°C, which was composed of two linear sections, showed good linear relationships; this indicated that the Avrami equation could properly describe the isothermal crystallization behavior of these samples.

Generally, the n value is used to roughly describe the nucleation mechanism and growth dimension. The n values of the neat PHBV and its blends were in the range 2.4–2.6 at 50°C. In general, $n = 3$ corresponded to two different kinds of possible crystallization mechanisms. One was three-dimensional growth and instantaneous nucleation; the other was two-dimensional growth and homogeneous nucleation. It was reported that PHBV melts are inclined to undergo homogeneous nucleation,[20] so the n value of PHBV close to 3 implied the crystallization mode of two-dimensional growth. To interpret n of the 6a-PLLA/PHBV blends, additional information on the morphology was measured by POM, as shown in Figure 3. 6a-PLLA decreased the size of the PHBV spherulites and increased the nucleation density by acting as a nucleating agent. We concluded that the nucleation mechanism of the neat PHBV and its blends were different, although their n values were similar. The n values ranged from 2.4 to 2.6 for the 6a-PLLA/PHBV blends and may have correspond to three-dimensional growth and instantaneous nucleation. The K values decreased with increasing content of 6a-PLLA; they exhibited similar trends to the values of the reciprocal of $t_{1/2}$.

We measured the spherulitic growth rate (G) of the PHBV component was measured by following the variation of radius of spherulites against t, and the values are listed in Table I. The G of PHBV decreased with increasing content of 6a-PLLA at 50°C. For the partially miscible 6a-PLLA/PHBV blends, part of the 6a-PLLA mixed with the PHBV component at a molecular level, whereas the others gathered into microdomains and separated homogeneously inside the PHBV phase.[17] Therefore, the well-mixed 6a-PLLA diluted the melt and retarded G of PHBV component. In combination with the increasing nucleation effect of 6a-PLLA on the crystallization of the PHBV component with increasing content of 6a-PLLA, as shown in Figure 3, the overall crystallization rate of the PHBV component first decreased and then increased when the 6a-PLLA content reached 60%.

The n values of the neat 6a-PLLA and its blends decreased gradually from 2.7 to 1.8 with increasing PHBV content when it was

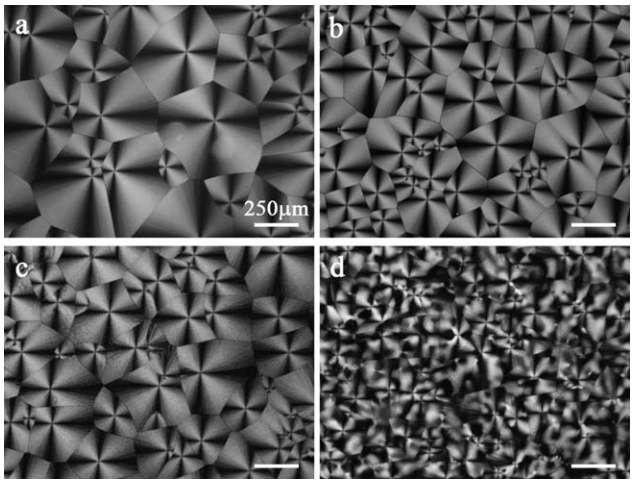

Figure 3. Spherulitic morphologies of the (a) neat PHBV, (b) 20/80 blend, (c) 40/60 blend, and (d) 60/40 blend crystallized at 50°C.

isothermally crystallized at 125°C. It is generally accepted that PLLA melts are inclined to undergo homogeneous nucleation.[21] So, the nucleation mode of 6a-PLLA was homogeneous nucleation with two-dimensional growth; this consistent with our earlier publication.[22] The spherulitic morphologies of the neat 6a-PLLA and its blends are shown in Figure 4. We observed that the spherulites of PLLA became larger, and the nucleation density decreased after blending with PHBV. In addition, the coarseness of the 6a-PLLA spherulites increased with increasing PHBV content. This indicated that PHBV was rejected into the interlamellar and interfibrillar regions of 6a-PLLA spherulites during the crystallization process; that is, the PHBV melt diluted the melt of 6a-PLLA. Thus, the decreased n value of blends resulted from the gradually decreased the growth dimension from two-dimensional growth to one-dimensional growth. The K values of these blends also exhibited similar trends as the values of $1/t_{1/2}$ except the 20/80 blend because of the much lower n value.

Except for the dilution effect, which could decrease the G of 6a-PLLA, the melt PHBV component improved the chain mobility of 6a-PLLA and facilitated crystallization. As a result, G of the 6a-PLLA spherulites, as shown in Table I, increased first and then decreased. However, the overall crystallization rate of the 6a-PLLA/PHBV blends kept decreasing with the increasing content of PHBV because of the decreasing nucleation density.

The n values of the neat 6a-PLLA and neat PHBV at 79°C were similar to those at lower and higher temperatures, respectively; this was indicative of the same crystallization mechanism at different T_cs. The crystallization mechanism of the 6a-PLLA/PHBV blends was complicated because of the simultaneous crystallization of both components. The plot of $\lg[-\ln(1-X_t)]$ against $\lg t$ of the 60/40 blend even showed two linear relationships. Although the n values (2.2–2.5) of these blends were similar to that of the neat PHBV, the crystallization mechanism was different. From the spherulitic morphology results shown in Figure 5, we found that the nucleation density of the PHBV spherulites increased when 20% 6a-PLLA was introduced; this indicated three-dimensional growth and instantaneous nucleation. For 6a-

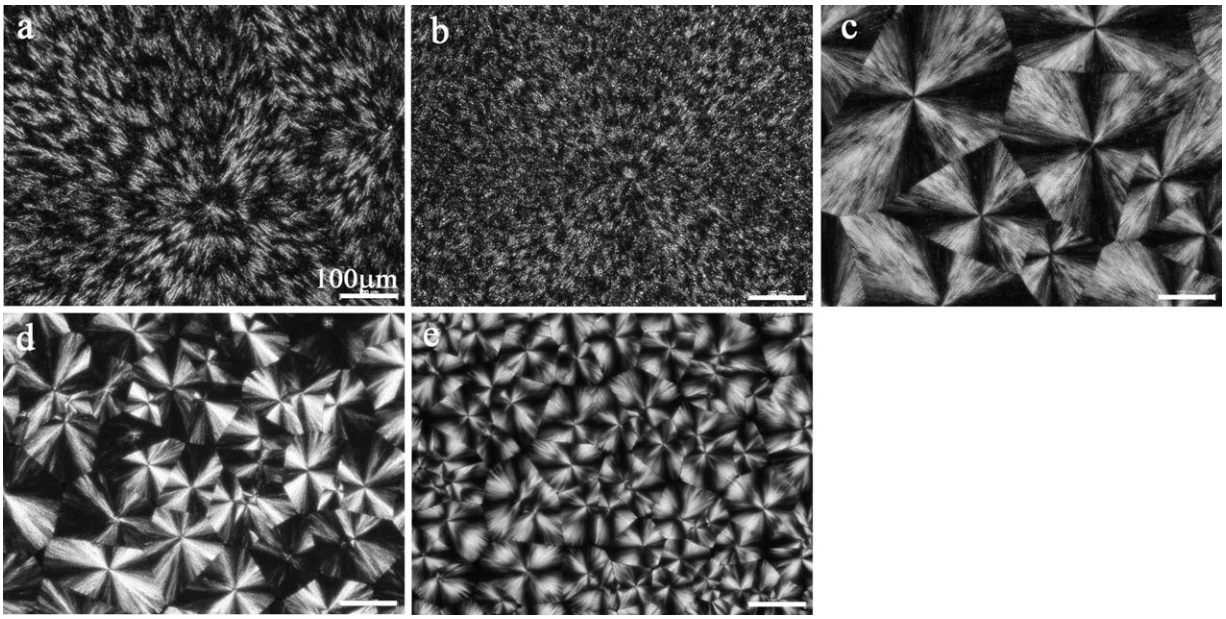

Figure 4. Spherulitic morphologies of the (a) 20/80 blend, (b) 40/60 blend, (c) 60/40 blend, (d) 80/20 blend, and (e) neat 6a-PLLA crystallized at 125°C.

PLLA/PHBV blends with a higher content of 6a-PLLA, the nucleation density of 6a-PLLA decreased, whereas the *n* value also decreased; this was similar to that crystallized at 125°C; this suggested that the crystallization mechanism of the 6a-PLLA component also changed to one-dimensional growth. We concluded that the crystallization mechanism of one component could be influenced by the other in the partially miscible 6a-PLLA/PHBV blends, no matter whether they crystallized simultaneously or not. In addition, *G* of the PHBV component in these blends had the same variation trend as those crystallized at 50°C and decreased with increasing content of 6a-PLLA.

Melting Behavior

The melting thermograms for the neat 6a-PLLA, neat PHBV, and their blends with various compositions after isothermal crystallization at 79 and 125°C are presented in Figure 6. As shown in Figure 6(a), the neat PHBV displayed double melting peaks with the high-temperature peak as the dominant one after

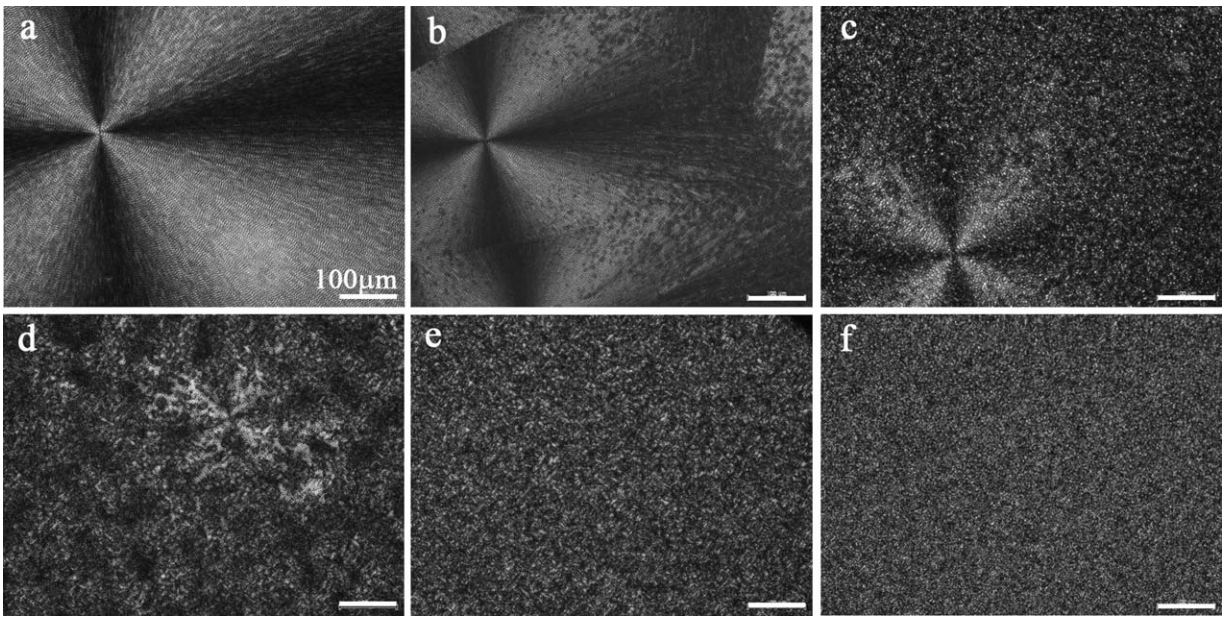

Figure 5. Spherulitic morphologies of the (a) neat PHBV, (b) 20/80 blend, (c) 40/60 blend, (d) 60/40 blend, (e) 80/20 blend, and (f) neat 6a-PLLA crystallized at 79°C.

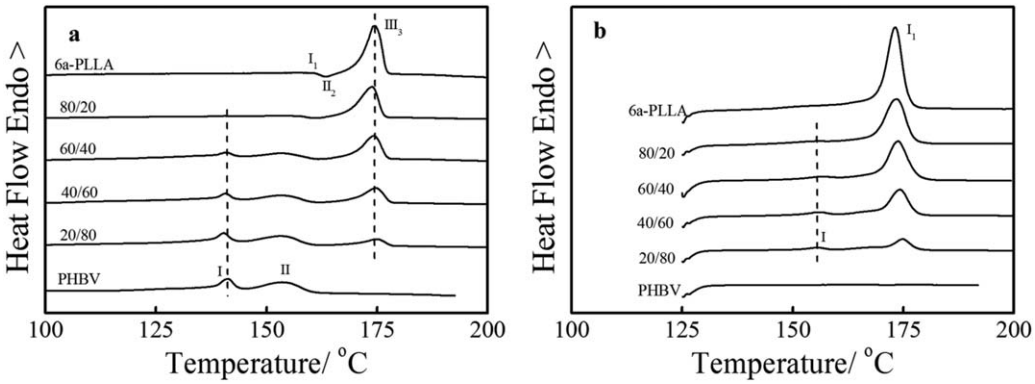

Figure 6. DSC melting curves of the 6a-PLLA/PHBV blends after isothermal crystallization at (a) 79 and (b) 125°C. The heating rates are (a) 5 and (b) 60°C/min, respectively.

melt crystallization at 79°C. This complex double melting behavior was due to the melting–recrystallization–remelting mechanism during heating.[23] For the neat 6a-PLLA, the melting curves showed three peaks: a small endothermic peak (I_1), an exothermic peak (II_2), and a final large fusion endothermic peak (III_3). In our previous work,[22] I_1 and II_2 were attributed to the fusion of imperfect crystals and the reorganization during heating process, respectively. III_3 refers to the perfected crystals formed during the reorganization process. As to the 6a-PLLA/PHBV blends, the double melting peaks (I and II) that were assigned to the PHBV component were found, and the enthalpy of fusion (ΔH_m) increased with increasing content of the PHBV component. I_1 and II_2 assigned to the 6a-PLLA component were not obvious because of overlapping with II and the lower content, but III_3 was clearly observed, and ΔH_m of this peak also increased with increasing content of 6a-PLLA. The melting results are consistent with the WAXD results.

At 125°C, it was difficult for neat PHBV to crystallize, so no melting peak was observed, even at a heating rate of 60°C/min after 1 h of crystallization. Neat 6a-PLLA displayed one melting peak at about 173°C. Except for the higher melting peak assigned to the PLLA component, it was interesting to find a very small I at about 156°C for the 6a-PLLA/PHBV blends, although no PHBV spherulites were found in the POM images under the same crystallization conditions. To clarify whether this peak was due to the PHBV component, the melting peaks of the 20/80 blend with different heating rates after crystallization at different T_cs for different times are shown in Figure 7.

As shown in Figure 7(a), there was no doubt that the melting peak I arose from the original crystallization of the PHBV component after crystallization at 79°C. Peak II arose from the recrystallized PHBV crystals and small amounts of 6a-PLLA imperfect crystals; this was be observed clearly from the tail of the melting peak II, as shown in Figure 7(b), at a heating rate of 60°C/min. t (15 min) was short, so the relative content of the PHBV crystals was low (see Figure 8); this was beneficial for detecting the melting peak of the 6a-PLLA component. With decreasing heating rate, the proportion between the enthalpy of I and II decreased [Figure 7(b)]. This was because the slow heating rate allowed the original crystal to have enough time to recrystallize. With increasing T_c, I shifted toward higher temperatures; this indicated that the small I for the samples crystallized at a higher T_c was from the melting of the PHBV crystals. This result suggests that the 6a-PLLA spherulite was favorable for the crystallization of the PHBV component. I_1 also shifted toward higher temperatures with increasing T_c. It is believed that I_1 arose from the melting of the 6a-PLLA crystals after crystallization at 125°C. To prove that I_1 after crystallization at lower temperatures but higher than 79°C also originated from the 6a-PLLA crystals, the melting peaks of a 20/80 6a-PLLA/PHBV blend after melt crystallization at 105°C for different times are shown in Figure 7(c). At the same heating rate, the lower

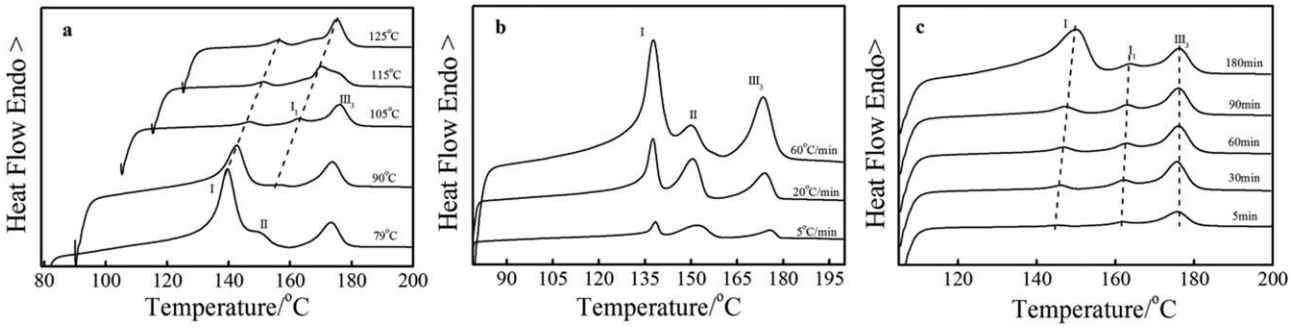

Figure 7. DSC melting curves of the 20/80 6a-PLLA/PHBV blend after isothermal crystallization at (a) different T_cs for 1 h with a heating rate of 60°C/min, (b) 79°C for 15 min with various heating rates, and (c) 105°C for different times with a heating rate of 60°C/min.

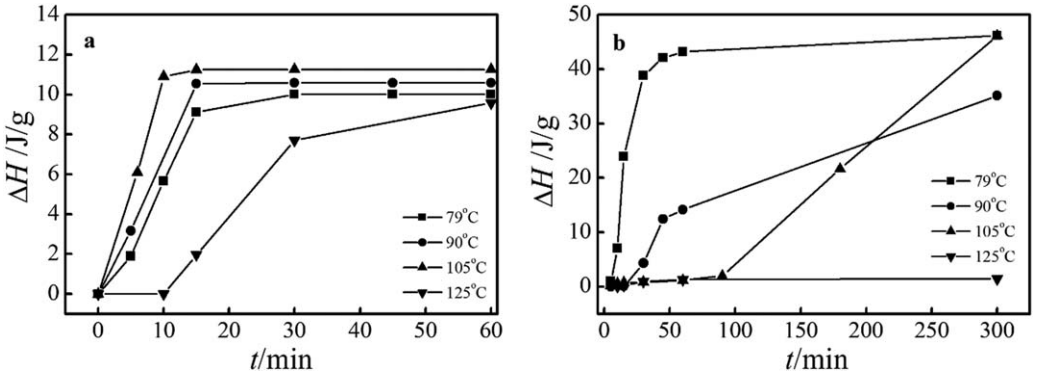

Figure 8. Plots of ΔH_m (ΔH) versus t after isothermal crystallization at various T_cs according to the DSC melting curves: (a) 6a-PLLA component and (b) PHBV component.

melting peak I associated with the PHBV component shifted toward higher temperatures, and the corresponding enthalpies showed an increase with increasing t; this suggested that more PHBV component crystallized, and they became more and more perfect. However, the enthalpies of I_1 and III_3 increased at first and then remained almost constant with increasing time. This indicated that the two peaks were the melting and remelting of the 6a-PLLA component and had no relationship to the PHBV component. In addition, we found that the enthalpy of melting peak I increased rapidly when t was over 90 min. It was reported in our previous article[16] that PHBV spherulites can crystallize inside the spherulites of 6a-PLLA after they fill the whole space. It was further proven that the melting peak I was from the PHBV crystals.

The plots of ΔH_m of the 6a-PLLA component and PHBV component versus t after crystallization at different T_cs are shown in Figure 8. From Figure 8(a), it can be seen clearly that ΔH_m of the 6a-PLLA component increased linearly with increasing time, for except crystallization at 125°C, which showed an induction time of about 10 min. After the induction time, a linear increase was also found. At the late period of the growth, ΔH_m no longer increased linearly but gradually reached a maximum. The crystal growth rate of the 6a-PLLA component was related to the slope of the linear increase. It was found that with the increase of T_c, the crystal growth rate increased first (it reached a maximum at 105°C) and then decreased. Compared with 6a-PLLA, the PHBV component needed a longer time to finish crystallizing. At 79°C, the contents of both the 6a-PLLA crystals and PHBV crystals increased with time within the first 15 min; this was concluded from the corresponding increased ΔH_ms, which indicated the simultaneous crystallization of both components. However, at higher T_cs, the induction time of the PHBV component was longer, so it began to crystallize after the completion of the crystallization of 6a-PLLA. The induction time of the PHBV component increased with increasing T_c. It was clear that the weak melting peak assigned to the PHBV component at 125°C resulted from the small quality of crystals formed during the induction time.

CONCLUSIONS

Except for the characteristic peaks of the neat 6a-PLLA and PHBV components, no new characteristic peaks were found from the WAXD patterns of the 6a-PLLA/PHBV blends; this indicated that the blending had no obvious effect upon the crystal structure of each component. The crystallization kinetics and spherulitic morphology results indicate that blending not only affected the crystallization mechanism but also had a complex influence on the overall crystallization rate of both components. Although the n values of the blends were similar to the neat PHBV component at lower T_cs, the crystallization mode of PHBV changed from two-dimensional and homogeneous nucleation for neat PHBV to three-dimensional and instantaneous nucleation for the blends. At higher T_cs, n decreased gradually; this indicated a decreasing growth dimension, which resulted from the dilution effect of the PHBV melt. The overall crystallization rate of the PHBV component was affected by two opposite effects from the 6a-PLLA component: the nucleation effect, which could accelerate the crystallization rate, and the dilution effect, which could impede crystal growth. Although the overall crystallization rate of the 6a-PLLA component was also affected by two things. On one hand, the melt PHBV component was unfavorable for the nucleation of the 6a-PLLA component. On the other hand, it improved the chain mobility of the 6a-PLLA component, which was beneficial to crystal growth. A weak melting peak assigned to the PHBV component was found in the blend after crystallization at higher temperatures; this was difficult for the crystallization of neat PHBV and suggested that the 6a-PLLA spherulite was favorable for the crystallization of the PHBV component. More studies with linear PLLA/PHBV with different miscibilities will be done to answer whether the miscibility and six-armed structure play important roles in all of these previous effects.

REFERENCES

1. Dodds, D. R.; Gross, R. A. *Science* **2007**, *318*, 1250.
2. Mohanty, A. K.; Misra, M.; Hinrichsen, G. *Macromol. Mater. Eng.* **2000**, *276/277*, 1.
3. Vilay, V.; Mariatti, M.; Ahmad, Z.; Pasomsouk, K.; Todo, M. J. *J. Appl. Polym. Sci.* **2009**, *114*, 1784.
4. Liu, H. Z.; Chen, F.; Liu, B.; Estep, G.; Zhang, J. W. *Macromolecules* **2010**, *43*, 6058.
5. Hsu, S. H.; Chen, W. C. *Biomaterials* **2000**, *21*, 359.
6. Jiang, S. H.; Wang, J.; Wu, J.; Chen, Y. C. *J. Appl. Polym. Sci.* **2015**, *132*, 41726.

7. Aluthge, D. C.; Xu, C.; Othman, N.; Noroozi, N.; Hatzikiriakos, S. G.; Mehrkhodavandi, P. *Macromolecules* **2013**, *46*, 3965.
8. Penning, J. P.; Manley, R. S. J. *Macromolecules* **1996**, *29*, 84.
9. Zhang, J. M.; Sato, H.; Furukawa, T.; Tsuji, H.; Noda, I.; Ozaki, Y. *Phys. Chem. B* **2006**, *110*, 24463.
10. Koyama, N.; Doi, Y. *Polymer* **1997**, *38*, 1589.
11. Furukawa, T.; Sato, H.; Murakami, R.; Zhang, J.; Duan, Y.; Noda, I.; Ochiai, S.; Ozaki, Y. *Macromolecules* **2005**, *38*, 6445.
12. Blümm, E.; Owen, A. J. *Polymer* **1995**, *36*, 4077.
13. Ikehara, T.; Kimura, H.; Qiu, Z. B. *Macromolecules* **2005**, *38*, 5104.
14. Run, M. T.; Wang, Y. G.; Yao, C. G.; Zhao, H. C. *J. Appl. Polym. Sci.* **2007**, *103*, 3316.
15. Chen, H. C.; Ma, C.; Bai, W.; Chen, D. L.; Xiong, C. D. *J. Macromol. Sci. Phys.* **2014**, *53*, 1715.
16. Jiang, N.; Abe, H. *Polymer* **2015**, *60*, 260.
17. Jiang, N.; Abe, H. *Polymer* **2015**, *66*, 259.
18. Galego, N.; Rozsa, C.; Sanchez, R. *Polym. Test.* **2000**, *19*, 485.
19. Zhang, J. M.; Duan, Y. X.; Sato, H.; Tsuji, H.; Noda, I.; Yan, S. K.; Ozaki, Y. *Macromolecules* **2005**, *38*, 8012.
20. Peng, S. W.; An, Y. X.; Chen, C.; Fei, B.; Zhuang, Y. G.; Dong, L. S. *Eur. Polym. J.* **2003**, *39*, 1475.
21. Miyata, T.; Masuko, T. *Polymer* **1998**, *39*, 5515.
22. Jiang, N.; Abe, H. *Polym. Degrad. Stab.* **2015**, *114*, 8.
23. Gunaratne, L.; Shanks, R. A. *Eur. Polym. J.* **2005**, *41*, 2980.